Bionanocomposites

DOI: 10.1002/anie.201004748

Artificial Nacre-like Bionanocomposite Films from the Self-Assembly of Chitosan–Montmorillonite Hybrid Building Blocks**

*Hong-Bin Yao, Zhi-Hua Tan, Hai-Yu Fang, and Shu-Hong Yu**

In the last decade, there has been a trend in chemistry to reduce the human impact on the environment.[1] Special attention has been paid to the replacement of conventional petroleum-based plastics by materials based on biopolymers.[2] However, the mechanical and thermal properties and functionalities of these biopolymers have to be enhanced to be competitive with the petroleum-based plastics from the viewpoint of practical applications. One of the most promising solutions to overcome these drawbacks is the elaboration of bionanocomposite, namely the dispersion of nanosized filler into a biopolymer matrix.[2,3]

Because of their functional properties, bionanocomposites as green nanocomposites based on biopolymers and layered silicates (clays) have received intensive attention in materials science.[3b,4] Chitosan and montmorillonite (MTM), an abundant polysaccharide and a natural clay respectively, have been widely used as the constituents of bionanocomposites.[5] The intercalation of chitosan into MTM and the dispersion of MTM nanosheets in the chitosan matrix have been systematically investigated.[6] Bionanocomposites based on chitosan intercalation into MTM can be used as a sensor applied in the potentiometric determination of several anions.[5a] Bionanocomposite films formed through the dispersion of MTM nanosheets in the chitosan matrix have shown enhancement of the mechanical and thermal properties compared with the pure chitosan film.[5c] Unfortunately, the enhancement of the tensile strength and thermal stability of the chitosan–MTM bionanocomposite film is still low far from the expectations in industry.

Systematic studies are carried out in materials science on natural materials with the objective of duplicating their properties in artificial materials.[7] Natural nanocomposites provide prime design models of lightweight, strong, stiff, and tough materials due to the hierarchical organization of the micro and nanostructures.[8] One attractive biological model for artificial material design is nacre (mother-of-pearl).[9] The microscopic architecture of nacre has been classically illustrated as a "brick-and-mortar" arrangement that plays an important role in the amazing mechanical properties of the nacre.[10] This arrangement is constituted of highly aligned inorganic aragonite platelets surrounded by a protein matrix, which serves as a glue between the platelets.[11]

Recently, the microstructure of the nacre has been mimicked by several innovative techniques to fabricate the artificial nacre-like materials with high mechanical performance. For example, layer-by-layer (LBL) deposition combining with cross-linking yielded poly(vinyl alcohol)/MTM nacre-like nanocomposites with a tensile strength of up to 400 MPa;[12] the ice-crystal templates of the microscopic layers were designed to form a brick-and-mortar microstructured Al_2O_3/poly(methyl methacrylate) composite that is 300 times tougher than its constituents;[13] the assembly of Al_2O_3 platelets on the air/water interface and sequent spin-coating was developed into the fabrication of lamellar Al_2O_3/chitosan hybrid films with high flaw tolerance and ductility;[14] the self-assembly of nanoclays with polymers coating by a paper-making method resulted in the nacre-mimetic films;[15] and nacre-like structural MTM–polyimide nanocomposites were fabricated by centrifugation deposition-assisted assembly.[16] Our group has also fabricated nacre-like chitosan-layered double hydroxide hybrid films with a tensile strength of up to 160MPa by sequential dipping coating and the LBL technique.[17] The concept of mimicking nacre and recently developed innovative techniques inspired us to fabricate the highly sustainable artificial nacre-like chitosan–MTM bionanocomposite film with high performance to seek a promising material for the replacement of conventional petroleum-based plastics.

Herein, we introduce a novel approach to fabricate artificial nacre-like chitosan–MTM bionanocomposite films by self-assembly of chitosan–MTM hybrid building blocks (Scheme 1). The chitosan molecules are very easily coated onto exfoliated MTM nanosheets to yield the hybrid building blocks by strong electrostatic and hydrogen-bonding interactions.[6] These hybrid building blocks can be dispersed in distilled water and then aligned to a nacre-like lamellar microstructure by vacuum-filtration- or water-evaporation-induced self-assembly because of the role that the orientation of the nanosheets and linking of the chitosan play.[18] The fabrication process is simple, fast, time-saving, and easily scaled up compared with the LBL,[12] ice-crystal-template,[13] and other techniques.[16]

[*] H. B. Yao, Z. H. Tan, H. Y. Fang, Prof. Dr. S. H. Yu
Division of Nanomaterials and Chemistry
Hefei National Laboratory for Physical Sciences at Microscale
Department of Chemistry
National Synchrotron Radiation Laboratory
University of Science and Technology of China
Hefei, Anhui 230026 (P.R. China)
Fax: (+86) 551-360-3040
E-mail: shyu@ustc.edu.cn
Homepage: http://staff.ustc.edu.cn/~yulab/

[**] S.H.Y. acknowledges the funding support from the National Basic Research Program of China (2010CB934700), the National Natural Science Foundation of China (Nos. 91022032, 50732006), and the International Science & Technology Cooperation Program of China (2010DFA41170).

Supporting information for this article is available on the WWW under http://dx.doi.org/10.1002/anie.201004748.

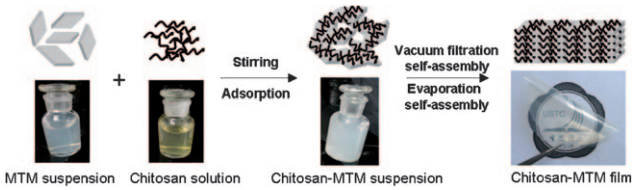

Scheme 1. Fabrication of the artificial nacre-like chitosan–MTM bionanocomposite film. Milky white colloidal chitosan–MTM hybrid building blocks were first prepared by mixing an aqueous suspension of exfoliated MTM nanosheet and an aqueous solution of chitosan and stirring to guarantee full adsorption of chitosan on MTM nanosheets. The chitosan–MTM hybrid building blocks were then aligned into the nacre-like structured composite by self-assembly induced by vacuum filtration or water evaporation.

At the first stage, the chitosan–MTM hybrid building blocks were prepared through mixing an aqueous suspension of exfoliated MTM nanosheets and an aqueous solution of chitosan. The resulting mixture was stirred for 12 h to allow the chitosan molecules to fully adsorb onto the surface of the MTM nanosheets. TEM images (Figure 1 a,b) confirm the sheet-like morphologies of both the MTM and chitosan–MTM, implying that chitosan–MTM is an ideal building block for fabricating lamellar microstructures.

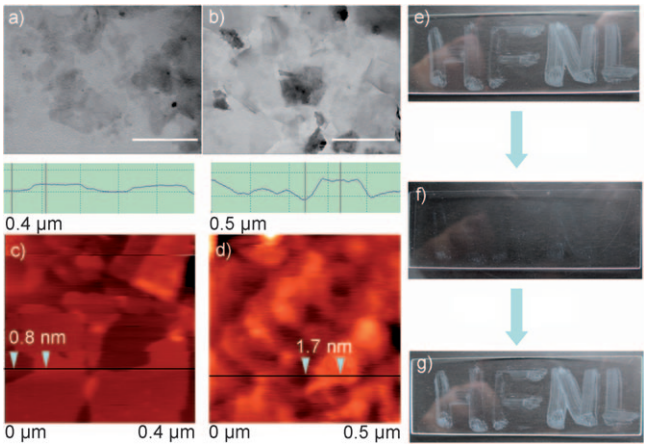

Figure 1. a,b) TEM images of MTM nanosheets before and after adsorbing chitosan molecules Scale bars: 500 nm. c,d) AFM images of MTM nanosheets corresponding to (a) and (b). e)–g) Photographs of patterns of chitosan–MTM as it is swollen in water (e→f) and dried (f→g).

The surface morphologies and the thickness of the MTM nanosheets before and after the adsorption of the chistosan molecules were characterized by AFM (Figure 1 c,d; Supporting Information, Figures S1, S2). The surface of the MTM nanosheets changed from smooth to rough and the average thickness increased from 0.97 to 1.98 nm, indicating that a total of about 1 nm-thick chitosan layers adsorbed on both sides of MTM nanosheets, which was confirmed by the TGA (Supporting Information, Figure S3). The adsorption of the chitosan molecules on the MTM nanosheets was also demonstrated by the FTIR spectra (Supporting Information, Figure S4): the adsorptions at 1556 and 1414 cm^{-1} can be designated as δ_{NH} and ν_{CN}, respectively. The MTM nanosheets with a chitosan coating were isolated by the centrifugation, washed with deionized water twice to remove unabsorbed chitosan, and finally collected as a glue-like substance. The obtained glue showed a strong adhesion and it can be painted on a glass slide (Figure 1 e). Interestingly, the chitosan–MTM patterns on the glass slide disappeared (Figure 1 f) under water due to the swelling. After the glass slide dried in the surrounding environment, the patterns would reappear as the original (Figure 1 g), indicating the adhesive properties of the hybrid building blocks even under the water.

The MTM nanosheets with chitosan coatings can be redispersed into deionized water, resulting in a milky white colloidal suspensionafter stirring and ultrasonication. The chitosan–MTM hybrid can then be easily used to fabricate the films with nacre-like lamellar microstructures by vacuum-filtration- or water-evaporation-induced self-assembly. Photographs of the obtained chitosan–MTM bionanocomposite films are shown in Figure 2, inset. These films are flexible,

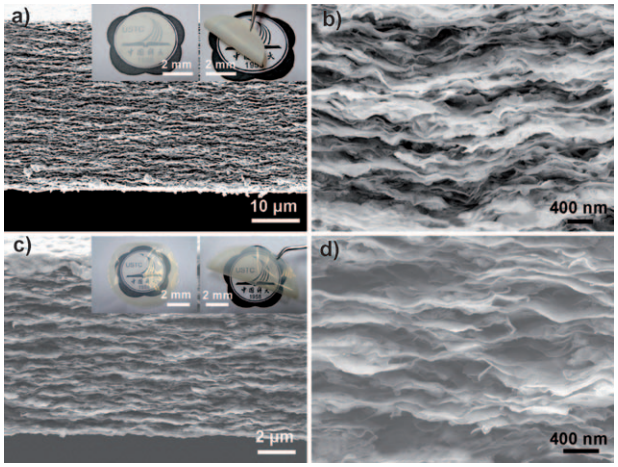

Figure 2. a,b) SEM images of a chitosan–MTM bionanocomposite film fabricated by vacuum filtration at different magnifications. c,d) A film fabricated by evaporation. Inserts in (a), (c): Photographs of the corresponding films.

glossy, and their surfaces are very smooth. The evaporation-induced film is more transparent than the film obtained by vacuum filtration owing to it being less thick. The microstructures of the fabricated films were observed by an SEM image in Figure 2. The chitosan–MTM hybrid building blocks are stacked together to form a densely oriented lamellar microstructure, which is reminiscent of the brick-and-mortar structure of nacre. Small-angle PXRD patterns also indicate the well-defined lamellar microstructures with a *d* spacing of 2.6 nm (Supporting Information, Figure S5). SEM images of the surfaces of the films reveal that the microstructures of the surface are flat, with only some nanoscale roughness (Supporting Information, Figure S6) that is slightly less in vacuum-filtration-induced composite films. The content of chitosan in these nacre-like bionanocomposite films was determined as 24 wt % by organic elemental analysis (Supporting Informa-

tion, Table S1), which is very low compared with that in traditional films.[5c] TGA analysis also indicated the low chitosan content (about 35 wt%; Supporting Information, Figure S3). The low organic constituent content in the obtained nacre-like chitosan–MTM bionanocomposite films is similar to that of the natural nacre.

Tensile-strength tests were carried on the chitosan–MTM films to show the role that the nacre brick-and-mortar microstructures play on the mechanical properties. A conventional film was prepared by simply mixing Na-MTM and chitosan together in aqueous solution and then allowing the film to form by evaporation. The microstructure of the contrast sample was checked without the brick-and-mortar microstructure by SEM (Supporting Information, Figure S7). The mechanic properties of the obtained samples are summarized in Table 1. Figure 3a shows that the ultimate

Table 1: Summary of the mechanical properties of films measured by tensile testing.

Samples	Young's modulus [GPa]	Ultimate stress [MPa]	Ultimate strain [%]
nacre-like chitosan–MTM film fabricated by vacuum filtration	10.7±1.7	76±10	0.97±0.14
nacre-like chitosan–MTM film fabricated by evaporation	6.8±1.6	99±13	2.32±0.39
conventional chitosan–MTM film fabricated by simply mixing	1.6±0.1	37±3.2	3.98±0.28

tensile strength of both the well-aligned artificial nacre-like films and conventional film. The mechanical performance of the well-aligned artificial nacre-like film is better than that of the film made by conventionally simply mixing the constituents. The Young's modulus and ultimate tensile strength of the well-aligned artificial nacre-like films are respectively 3–5-fold and 2–3-fold higher than that of the conventional film.

An atomic modeling (Figure 3b) was used to investigate the mechanical properties at the molecular scale. The modeling shows that the geometry of SiO_4 tetrahedrons on the surface of the MTM is conductive to cooperative hydrogen bonding. On the chain of the chitosan molecules, there are many OH and NH_3 groups, which are likely to form the hydrogen bonding with SiO_4 tetrahedrons on the surface of the MTM when the chitosan chains are close to the surface of MTM under the electrostatic attraction. On the other hand, the stereochemistry of the six rings in the chitosan chain is an obstacle to the hydrogen bonding formation of some OH and NH_3 groups with SiO_4 tetrahedra. Moreover, we did not observe Al–O–C bond formation in the FT-IR spectra; PVA molecules can form Al–O–C bonds, as reported by Kotov et al.[12b] Thus, it is reasonable that the chitosan–MTM films can not achieve mechanical strengths that are as high as PVA–MTM films.[12b] However, the hydrogen bonding and the lamellar structure can contribute to a higher mechanical performance compared with the conventional chitosan–MTM films.

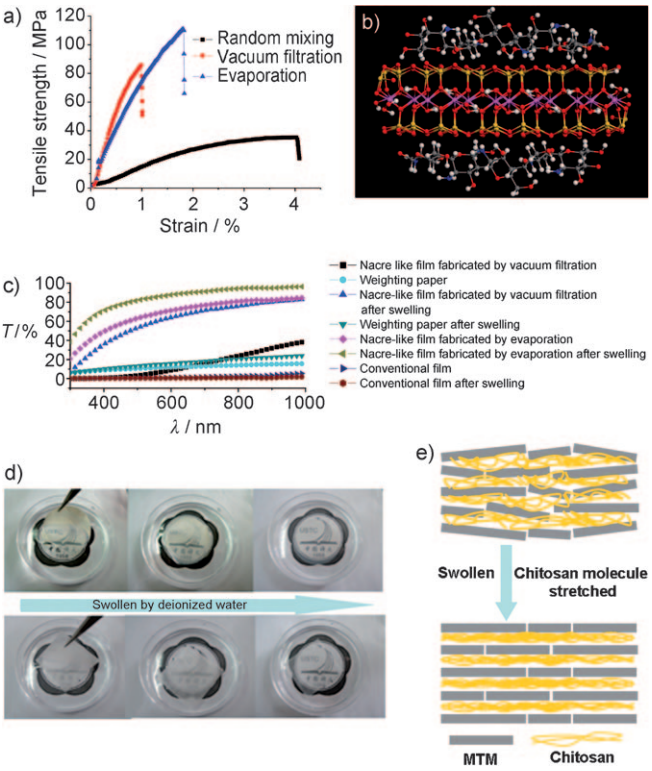

Figure 3. a) Tensile strength–strain curves for chitosan–MTM bionanocomposite films obtained by different methods. b) Atomic modeling of the chitosan molecules adsorbing on the MTM surface. The model was constructed using Material Studio software (version 4.1) and the geometry optimization of the model was calculated by the Forcite tool. Al purple, Si yellow, O red, C gray, N blue, H white. c) UV/Vis transmittance spectra of different samples before and after swelling with water. d) Photographs of nacre-like bionanocomposite film (top) and weighting paper (bottom) during the water swelling process. e) Models of the nacre-like chitosan–MTM bionanocomposite film before and after swelling by water.

The well-aligned lamellar microstructures also lead to a good light transmittance of the films. Because of the high orientation of the chitosan–MTM hybrid building blocks, which greatly decreases the light scattering between the nanosheets, the obtained chitosan–MTM films were more transparent than conventional chitosan–MTM films in which the MTM nanosheets are randomly dispersed. The transmittance spectra (Figure 3c) show about 60–80% transparence across the visible spectrum of light for the evaporation induced chitosan–MTM film, in contrast to only 2–3% for the conventional film. Interestingly, when the chitosan–MTM films were swollen by water, their transparence was further enhanced, in contrast to a small increase for that of conventional films. There are two main reasons leading to the enhancement of transparence of nacre-like films, which almost completely disappeared in water (Figure 3d). One reason is the common physical phenomenon that when water fills the space, the light scattering occurring at the interfaces would decrease because the refractive index of water is more similar to that of the solid material than to that of air. We used weighing paper as the contrast sample to show how this effect occurred on the increase of transparence of the film (Fig-

ure 3d), and transmittance spectra indicate that such an increase is limited (Figure 3c). The other reason is that the lamellar microstructures of the nacre-like films lead to the increase of transparence. After water swelling, the chitosan molecules between the MTM nanosheets stretched to optimize the lamellar microstructures, which largely decreased the light scattering between the MTM nanosheet interfaces (Figure 3e). The optimization of lamellar microstructures contributed to a 20–30% increase of transparence across the visible spectrum for the vacuum-filtration-induced chitosan–MTM film.

LBL assembled lamellar structural polyelectrolyte–clay coatings on fabric have shown high efficient fire retardancy.[19] The fire retardancy of the vacuum-filtration-induced chitosan–MTM film was tested because of its considerable thickness (see video provided in the Supporting Information). When exposed to the flame of blast burner, the film initially burnt very briefly owing to the small amount of the chitosan adsorbed on the MTM nanosheets, and the film gradually became black, which was partly induced by carbonization of the chitosan. After burning out the chitosan, the MTM nanosheets do not support any burning and remain inert under prolonged exposure to the flame (Figure 4b, inset).

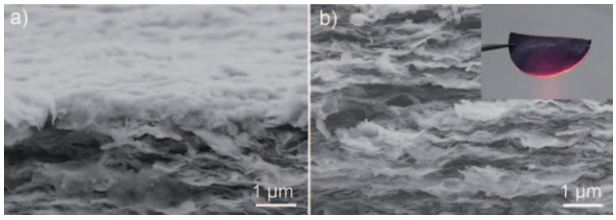

Figure 4. SEM images of the nacre-like chitosan–MTM bionanocomposite film after burning: a) The surface of the film; b) the inside structure of the film. Insert in (b) shows the film being exposed to the flame.

Furthermore, burning the film never lead to any dripping of hot fluids such as for plastic films, and the shape of the film was maintained even with constant exposure to the flame of a blast burner. The microstructures of the film after burning were checked by SEM, and the images showed that a flame-protective cuticle of tightly condensed nanoclay formed (Figure 4a) and the nacre-like lamellar microstructures were still maintained inside the film (Figure 4b).

In summary, hybrid building blocks with a thin layer of chitosan coating on the MTM nanosheets can be conveniently prepared and self-assembled to form chitosan–MTM bionanocomposite films by vacuum filtration or water evaporation. The MTM–chitosan hybrid nanosheets were characterized by the AFM, FTIR, and TGA; these methods indicate that about 1 nm-thick total chitosan molecules were adsorbed on both sides of MTM nanosheets. The obtained bionanocomposite films have a nacre-like brick-and-mortar micostructure, which leads to their high performances in mechanical properties, light transmittance, and fire resistant properties. The Young's modulus and ultimate tensile strength of the well-aligned artificial nacre-like films are 3–5-fold and 2–3-fold higher than that of films fabricated by conventional methods. The chitosan–MTM film has 60–80% transparency across the visible spectrum, compared to 2–3% of that of the conventional films. The chitosan–MTM films can maintain their self-supported shapes under the constant exposure to flame of blast burner. The present facile fabrication process is expected to allow the design and preparation of different biomimetic nanocomposites with unique functionalities with improved performances.

Experimental Section

Chitosan and glacial acetic acid were purchased from Sinopharm Chemical Reagent Co. Ltd. Sodium montmorillonite (Na-MTM) nanoclays were offered by Zhejiang Fenghong Clay Co. Ltd. All chemicals were analytical grade and used as received without further purification.

Preparation of chitosan–MTM hybrid nanosheets: A dispersion of Na-MTM in deionized water (0.5 wt%) was stirred thoroughly for one week and then centrifuged at 3000 rpm for 10 min to remove unexfoliated Na-MTM. Chitosan (2 wt%) was dissolved in an aqueous solution of 2 wt.% glacial acetic acid 24 hours before use. The same volume of the exfoliated Na-MTM solution and chitosan solution (2 wt%) were mixed under the constant stirring for 24 h to guarantee the full adsorption of chitosan on MTM nanosheets. The chitosan-coated MTM hybrid nanosheets were collected by centrifugation at 9000 rpm for 10 min, washed by deionized water twice to remove the unabsorbed chitosan, and finally collected as a glue-like substance.

Nacre-like chitosan–MTM bionanocomposite films were fabricated by two different self-assembly procedures**:** A desired amount of chitosan–MTM glue was dispersed into deionized water (20 mL) under ultrasonication. 1) Vacuum-filtration-induced self-assembly: The obtained suspension was vacuum filtered to form nacre-like chitosan–MTM bionanocomposite film on the cellulose acetate filtration paper, with pore size of 0.2 μm, and then dried in a 60°C oven. Freestanding films were obtained by dissolving the cellulose acetate filtration paper in acetone. 2) Water-evaporation-induced self-assembly: The obtained suspension was poured into the Petri dish and kept in the 60°C oven for evaporation to form nacre-like chitosan–MTM bionanocomposite film on the bottom of the Petri dish. Freestanding films were obtained by directly peeling off from the bottom of the Petri dish.

Fabrication of conventional film: In a typical procedure, Na-MTM (3 g) was dispersed into chitosan solution (2 wt%, 50 mL) under constant stirring for 24 h and the suspension was set for several hours. The suspension (20 mL) was then poured into the Petri dish and kept in a 60°C oven to evaporate and form the chitosan–MTM bionanocomposite film on the bottom of the Petri dish. The freestanding film was peeled off from the bottom of the Petri dish.

X-ray powder diffraction(PXRD) patterns were obtained with a Japan Rigaku DMax-γA rotation-anode X-ray diffractometer equipped with graphite-monochromatized Cu-K radiation ($\lambda =$ 1.54178 Å). Transmission electron microscope (TEM) images were taken with a Hitachi H-7650 transmission electron microscope at an acceleration voltage of 120 kV. Atomic force microscope (AFM) images were carried out by Vecco di Innova. A freshly cleaved mica slide was used as the substrate for the AFM measurement and one drop of the dilute solution of sample (0.5 wt%) was dropped on the substrate and dried naturally for the AFM characterization. Scanning electron microscope (SEM) images were taken with a Zeiss Supra 40 scanning electron microscope at an acceleration voltage of 5 kV. The UV/Vis transmittance spectra of the films were collected on SHIMADZU DUV-3700. Thermal gravimetric analysis (TGA) was carried out with a TA SDT Q600 thermal analyzer, with a heating rate of 10°C min^{-1} under air. The mechanical properties of freestanding

films were measured under tensile mode in a universal mechanical testing machine (Instron 5565 A) . For the mechanical testing, the films were cut with a razor blade into rectangle bars of approximate length 23 mm and width 5 mm; the distance between the clamps was 5 mm and the load speed was 10 mm min^{-1}.

The Supporting Information contains AFM images, elemental analysis, FT-IR spectra, PXRD patterns, SEM images, and videos.

Received: July 31, 2010
Revised: October 4, 2010
Published online: November 25, 2010

Keywords: biomimetics · bionanocomposites · chitosan · montmorillonite · nacre-like structures

[1] R. A. Gross, B. Kalra, *Science* **2002**, *297*, 803.
[2] F. Chivrac, E. Pollet, L. Avérous, *Mater. Sci. Eng. R* **2009**, *67*, 1.
[3] a) B. Chen, J. R. G. Evans, H. C. Greenwell, P. Boulet, P. V. Coveney, A. A. Bowden, A. Whiting, *Chem. Soc. Rev.* **2008**, *37*, 568; b) E. Ruiz-Hitzky, M. Darder, P. Aranda, *J. Mater. Chem.* **2005**, *15*, 3650; c) M. Alexandre, P. Dubois, *Mater. Sci. Eng. R* **2000**, *28*, 1; d) B. Chen, J. R. G. Evans, *Soft Matter* **2009**, *5*, 3572; e) M. Darder, P. Aranda, E. Ruiz-Hitzky, *Adv. Mater.* **2007**, *19*, 1309; f) N. Sheng, M. C. Boyce, D. M. Parks, G. C. Rutledge, J. I. Abes, R. E. Cohen, *Polymer* **2004**, *45*, 487.
[4] S. Sinha Ray, M. Bousmina, *Prog. Mater. Sci.* **2005**, *50*, 962.
[5] a) M. Darder, M. Colilla, E. Ruiz-Hitzky, *Chem. Mater.* **2003**, *15*, 3774; b) J.-W. Rhim, S.-I. Hong, H.-M. Park, P. K. W. Ng, *J. Agric. Food Chem.* **2006**, *54*, 5814; c) Y. Xu, X. Ren, M. A. Hanna, *J. Appl. Polym. Sci.* **2006**, *99*, 1684.
[6] Y. Shchipunov, N. Ivanova, V. Silant′ev, *Green Chem.* **2009**, *11*, 1758.
[7] a) B. Bhushan, *Philos. Trans. R. Soc. London Ser. A* **2009**, *367*, 1445; b) P. Fratzl, *J. R. Soc. Interface* **2007**, *4*, 637; c) C. Sanchez, H. Arribart, M. M. Giraud Guille, *Nat. Mater.* **2005**, *4*, 277; d) E. Dujardin, S. Mann, *Adv. Mater.* **2002**, *14*, 775.
[8] M. A. Meyers, P.-Y. Chen, A. Y.-M. Lin, Y. Seki, *Prog. Mater. Sci.* **2008**, *53*, 1.
[9] G. M. Luz, J. F. Mano, *Philos. Trans. R. Soc. London Ser. A* **2009**, *367*, 1587.
[10] A. P. Jackson, J. F. V. Vincent, R. M. Turner, *Proc. R. Soc. London Ser. B* **1988**, *234*, 415.
[11] a) F. Song, A. K. Soh, Y. L. Bai, *Biomaterials* **2003**, *24*, 3623; b) X. Li, W.-C. Chang, Y. J. Chao, R. Wang, M. Chang, *Nano Lett.* **2004**, *4*, 613.
[12] a) Z. Tang, N. A. Kotov, S. Magonov, B. Ozturk, *Nat. Mater.* **2003**, *2*, 413; b) P. Podsiadlo, A. K. Kaushik, E. M. Arruda, A. M. Waas, B. S. Shim, J. Xu, H. Nandivada, B. G. Pumplin, J. Lahann, A. Ramamoorthy, N. A. Kotov, *Science* **2007**, *318*, 80.
[13] a) S. Deville, E. Saiz, R. K. Nalla, A. P. Tomsia, *Science* **2006**, *311*, 515; b) E. Munch, M. E. Launey, D. H. Alsem, E. Saiz, A. P. Tomsia, R. O. Ritchie, *Science* **2008**, *322*, 1516.
[14] L. J. Bonderer, A. R. Studart, L. J. Gauckler, *Science* **2008**, *319*, 1069.
[15] a) A. Walther, I. Bjurhager, J.-M. Malho, J. Pere, J. Ruokolainen, L. A. Berglund, O. Ikkala, *Nano Lett.* **2010**, *10*, 2742; b) A. Walther, I. Bjurhager, J. M. Malho, J. Ruokolainen, L. Berglund, O. Ikkala, *Angew. Chem.* **2010**, *122*, 6593; *Angew. Chem. Int. Ed.* **2010**, *49*, 6448.
[16] R. Chen, C.-a. Wang, Y. Huang, H. Le, *Mater. Sci. Eng. C* **2008**, *28*, 218.
[17] H. B. Yao, H. Y. Fang, Z. H. Tan, L. H. Wu, S. H. Yu, *Angew. Chem.* **2010**, *122*, 2186; *Angew. Chem. Int. Ed.* **2010**, *49*, 2140.
[18] a) T. Liu, et al., *Bioinspiration Biomimetics* **2008**, *3*, 016005; b) B. V. Lotsch, G. A. Ozin, *J. Am. Chem. Soc.* **2008**, *130*, 15252.
[19] a) Y.-C. Li, J. Schulz, J. C. Grunlan, *ACS Appl. Mater. Interfaces* **2009**, *1*, 2338; b) Y.-C. Li, J. Schulz, S. Mannen, C. Delhom, B. Condon, S. Chang, M. Zammarano, J. C. Grunlan, *ACS Nano* **2010**, *4*, 3325.

